doi:10.1111/evo.1404

Interspecific allometry for sexual shape dimorphism: Macroevolution of multivariate sexual phenotypes with application to Rensch's rule

Dean C. Adams,[1,2] Elizabeth Glynne,[1] and Antigoni Kaliontzopoulou[3]

[1] *Department of Ecology, Evolution, and Organismal Biology, Iowa State University, Ames, Iowa 50011*

[2] *E-mail: dcadams@iastate.edu*

[3] *CIBIO Research Centre in Biodiversity and Genetic Resources, InBIO, Universidade do Porto, Campus de Vairão, Vila do Conde, Porto 4099-002, Portugal*

Received March 19, 2020

Accepted June 19, 2020

Allometric trends in the degree of sexual dimorphism with body size have long fascinated evolutionary biologists. Many male-biased clades display more prominent sexual dimorphism in larger taxa (Rensch's rule), with most examples documenting this pattern for body size dimorphism. Although sexual dimorphism in traits other than body size is equally functionally relevant, characterizing allometric patterns of sexual dimorphism in such traits is hampered by lack of an analytical framework that can accommodate multivariate phenotypes. In this article, we derive a multivariate equivalency for investigating trends in sexual dimorphism—relative to overall body size—across taxa and provide a generalized test to determine whether such allometric patterns correspond with Rensch's rule. For univariate linear traits such as body size, our approach yields equivalent results to those from standard procedures, but our test is also capable of detecting trends in multivariate datasets such as shape. Computer simulations reveal that the method displays appropriate statistical properties, and an empirical example in Mediterranean lizards provides the first demonstration of Rensch's rule in a multivariate phenotype (head shape). Our generalized procedure substantially extends the analytical toolkit for investigating macroevolutionary patterns of sexual dimorphism and seeking a better understanding of the processes that underlie them.

KEY WORDS: Morphological evolution, multivariate, sexual dimorphism.

> Thus, the rule is valid that in numerous animal groups the sexual dimorphism increases with body size… If by way of exception, the females are larger than the males, the opposite correlation applies, i.e., the greater sexual difference is found in the smaller species. (Rensch 1960, pp. 157, 159)

It is widely observed that males and females of the same species are not identical, but rather differ—sometimes substantially—in their phenotypic characteristics (Fairbairn 1997, 2013). Indeed, sexual dimorphism is pervasive across many animal clades, and understanding the causes for this pattern has attracted considerable attention in evolutionary biology for well over a century (e.g., Darwin 1871; Fairbairn et al. 2007). One of the most conspicuous differences between males and females is their body sizes (Andersson 1994), where sexual divergence is often hypothesized to be the result of selection pressures related to reproduction, or the distinct ecological roles of males and females in their respective habitat (Cox et al. 2003; Stephens and Wiens 2009; Kaliontzopoulou et al. 2015; Tarr et al. 2018; Littleford-Colquhoun et al. 2019). For example, both sexual selection on male body size (Cox et al. 2003; Garcia-Navas et al. 2015; Horne et al. 2020) and fecundity selection on female body size (Serrano-Meneses and Szekely 2006; Stuart-Fox 2008) are expected to enhance the degree of sexual size dimorphism (SSD) in taxa over evolutionary time. Likewise, when males and

© 2020 The Authors. *Evolution* © 2020 The Society for the Study of Evolution.

females respond differently to environmental factors, intraspecific competition may generate ecological divergence between them, resulting in varying patterns of sexual dimorphism (Butler et al. 2000; Bolnick and Doebeli 2003; Dayan and Simberloff 2005; Kaliontzopoulou et al. 2010; Meiri et al. 2014).

Patterns of sexual differentiation, and variation in those patterns across taxa, are not restricted to body size alone but are also expressed in the relative proportions of structures, their shape, and other properties of different body parts and traits. Additionally, sexual differences in these traits, which are critical to organismal function and survival, may also be the result both sexual and natural selective mechanisms. As such, the investigation of variation between the sexes in body form can shed light both on their respective reproductive and social functions (Kaliontzopoulou et al. 2007) and their ecological roles (Butler and Losos 2002; Kaliontzopoulou et al. 2010). Several studies have documented patterns of sexual dimorphism in body proportions (e.g., Butler and Losos 2002; Butler et al. 2007; Kaliontzopoulou et al. 2015), the shape of various structures (e.g., Gidaszewski et al. 2009; Kaliontzopoulou et al. 2012; Berns and Adams 2013; Kelly et al. 2013; Sanger et al. 2013; Laporte et al. 2017; Law and Mehta 2018), ornamentation (e.g., Geist and Bayer 1988; Emlen 2008; Watson and Simmons 2010), or coloration (e.g., Endler 1983) to provide insights regarding the selective mechanisms that generate such patterns in nature. From a methodological perspective, sexual dimorphism in complex traits is typically quantified using multivariate approaches that fully integrate information on different aspects of the phenotype (Wyman et al. 2013). Indeed, understanding phenotypic evolution is inherently a multivariate endeavor (Blows 2007; Collyer et al. 2015; Adams and Collyer 2018, 2019), as processes such as natural and sexual selection simultaneously operate on more than one trait (Lande 1979; Lande and Arnold 1983). Additionally, the investigation of sexual dimorphism in traits other than body size is frequently linked to the analysis of intraspecific allometries, and differences in the allometric trajectories between males and females (De Lisle and Rowe 2013; Sanger et al. 2013; Kaliontzopoulou et al. 2015). Here it is hypothesized that differential allometry between males and females may point to the proximate and evolutionary mechanisms that control sexual dimorphism, such as sexual bimaturation and differential investment to growth (in the case of ontogenetic allometry), or to the exaggeration of sexually selected traits (in the case of static allometry) (i.e., Badyaev 2002; Butler and Losos 2002; De Lisle and Rowe 2013).

At macroevolutionary scales, changes in the relative contribution of selective forces may create variation in the degree of sexual dimorphism displayed across closely related taxa. For instance, sister species inhabiting different environments, or possessing distinct ecological adaptations, may exhibit differing degrees of sexual dimorphism as a result of differences in the balance of intensity between natural and sexual selection (Blanckenhorn et al. 2006; Stuart-Fox and Moussalli 2007; Östman and Stuart-Fox 2011; Kaliontzopoulou et al. 2015; see also Punzalan and Rowe 2015). Notably, such variation in the magnitude of sexual dimorphism may be in part mediated, though not obligatorily linked, to variation in intraspecific allometries. For instance, the patterns of intraspecific static allometry in sexually selected traits establishes a relationship between variation in those traits relative to size, and the evolutionary allometry across taxa in the degree of sexual dimorphism that may be expected (Rensch 1960; Reiss 1986; De Lisle and Rowe 2013; but see Bonduriansky 2007). When considered from this perspective, the "exaggeration" of body structures with increasing body size is predicted to generate an allometric trend in the degree of sexual dimorphism relative to overall body size across taxa.

Allometric patterns in the degree of sexual dimorphism relative to overall body size have long been posited to be a pervasive macroevolutionary trend. For instance, Rensch (1950, 1960) noted that in species where males are the larger sex, the degree of sexual dimorphism often increases with an increase in species' average body size (Rensch 1950; Abouheif and Fairbairn 1997; Fairbairn 1997). Likewise, in species where females are the larger sex, the degree of sexual dimorphism often increases with decreasing body size (Rensch 1960). Such interspecific patterns in the allometry of sexual dimorphism are termed *Rensch's rule*. Empirical studies have documented macroevolutionary trends in SSD consistent with Rensch's rule in a wide variety of animal taxa (Dale et al. 2007; Ceballos et al. 2013; Regis and Meik 2017; Johnson et al. 2017). However, other clades display the converse trend (Burbrink and Futterman 2019; Peñalver-Alcázar et al. 2019), and some clades display no relationship between SSD and body size (Astúa 2010; Hirst and Kiørboe 2014; Johnson et al. 2017). From an evolutionary perspective, the association between SSD and body size has been hypothesized to be driven by variation in ontogenetic or static allometries across taxa, which results from the influence of sex-specific selection on growth and maturation patterns (Rensch 1960; Dale et al. 2007), with relevance for both body size and the allometric growth of other traits.

Interestingly, virtually all evaluations of allometric patterns of the degree of sexual dimorphism across taxa have investigated patterns of size dimorphism, yet Rensch's original contributions were concerned with a much wider array of phenotypic traits that can differ between the sexes. These included not only sexual differences in body size, but also in general body proportions (e.g., relative wing and limb lengths), the degree of complexity of different body structures, the presence of sex-specific ornamentation (e.g., horns, body coloration, etc.), and other sex-specific differences (Rensch 1950, 1960). Thus, in this regard Rensch's (1950) vision was far more synthetic, as he sought to explain the

extent to which sexual dimorphism – across a general suite of phenotypic characteristics—scaled with overall body size in organisms, and why some species displayed a greater degree of sexual dimorphism than did others. However, despite both this clear prediction and Rensch's original observations, the evolutionary scaling of the degree of sexual dimorphism in phenotypic traits other than size remains largely unexplored (but see, e.g., Blanckenhorn et al. 2007). One possible reason for this disconnect is that to interrogate such patterns in complex multivariate traits, one requires analytical procedures that can accommodate multidimensional datasets in the evaluation of such trends. Further, while some have examined whether differences in the degree of SSD contribute to overall levels of sexual shape dimorphism (SShD) within and among taxa (O'Higgins et al. 1990), or have partitioned SShD into its size-related and unrelated components (Gidaszewski et al. 2009), no study has examined explicitly whether the degree of SShD changes systematically with changes in body size across taxa. In other words, no study has examined whether interspecific allometry for the degree of SShD relative to overall size exhibits trends in accordance with Rensch's observations.

In this article, we derive a multivariate equivalency for inspecting variation in sexual dimorphism—relative to overall body size—across taxa, and provide a generalized test to determine whether such patterns are consistent with Rensch's rule. Our procedure is appropriate for evaluating trends in univariate traits measured on a linear scale (such as body size or relative limb length), as well as in multivariate datasets representing complex phenotypes (such as sets of body proportions or landmark-based shape data). Thus, our procedure is capable of evaluating allometric trends of sexual dimorphism among taxa in all manner of phenotypic traits (Fig. 1). For univariate data, the approach yields equivalent results to what is normally accomplished for evaluations of SSD. However, the approach extends these procedures for the examination of sexual dimorphism in multivariate data, thereby increasing the potential for our conceptual understanding of the consequences of sexual and natural selection on complex organismal phenotypes. We conduct a series of computer simulations demonstrating that the approach displays appropriate statistical properties when evaluating trends in both univariate and multivariate data. We also provide an empirical example in Mediterranean green lizards, which illustrates the efficacy of our approach on both univariate and multivariate datasets. Finally, we highlight the new avenues of evolutionary research that our generalization facilitates, and make comments on the prospects for future empirical advances.

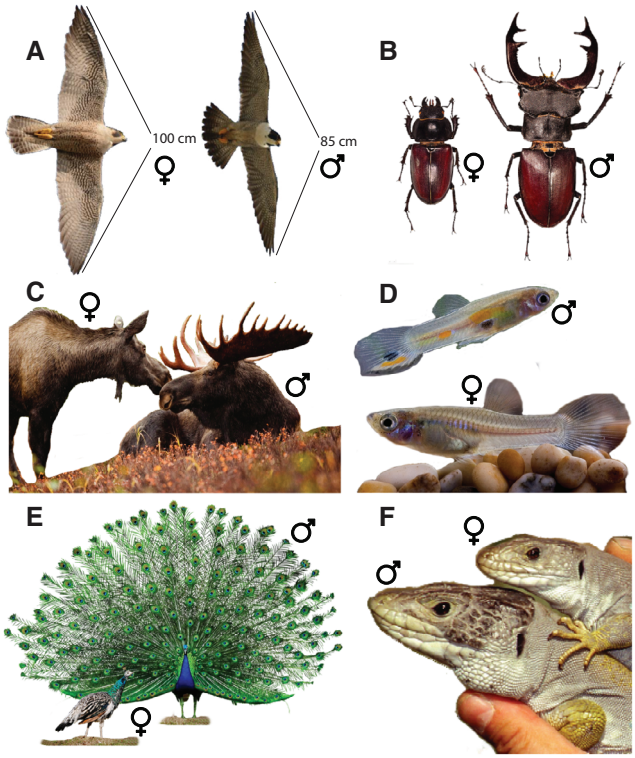


Figure 1. Visualization of some aspects of sexual dimorphism commonly displayed among animals, and for which the approach developed here, may be used to examine patterns across taxa. (A) Sexual size dimorphism (photos by Don Endicott and Patricia Simpson), (B) sexual dimorphism in the complexity of anatomical structures (photo by Didier Descouens), (C, D) sexual dimorphism in sex-specific ornamentation (photo by Per Harald Olsen), (E) sexual dimorphism in behavior, and (F) sexual shape dimorphism (photo by Bernard Dupont). Images A,B,D, E, and F are Creative Commons license; image C is from Wikimedia commons.

Methods and Results

ANALYTICAL DEVELOPMENT

To accommodate multivariate data in tests that evaluate interspecific trends in sexually dimorphic phenotypes, we must first derive a series of mathematical equivalencies based on how interspecific patterns of SSD are typically evaluated. For SSD, interspecific patterns are often inspected using a bivariate log-log plot, where the size of one sex is plotted against the size of the other sex (e.g., Fairbairn and Preziosi 1994; Abouheif and Fairbairn 1997; Ceballos et al. 2013). An example with simulated data is shown in Figure 2A, with the log of male size plotted against the log of female size. The diagonal line represents no size dimorphism; or a 1:1 size ratio between the sexes across the range of body sizes for species in the clade of interest. In this construction, deviations from the 1:1 line represent differential trends in SSD across taxa. For instance, trends that are parallel to the 1:1 line but are above or below it represent clades where all species display a similar amount of sexual dimorphism (i.e., the same absolute magnitude of sexual difference). Alternatively, trends that are steeper or shallower than the 1:1 line represent clades where one sex becomes disproportionately larger or smaller than

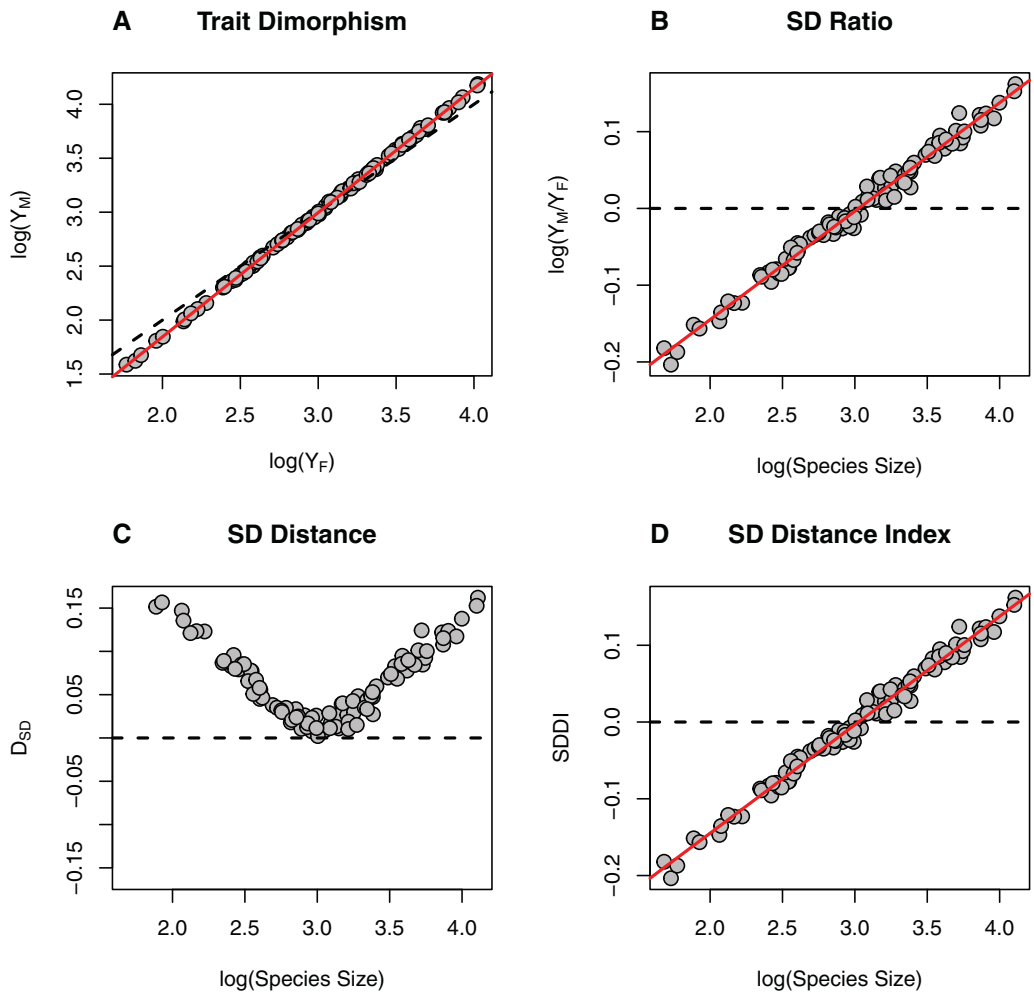


Figure 2. **Patterns of sexual size dimorphism across 100 hypothetical species. (A) The log-log plot of male versus female size exhibits a slope greater than one (β > 1.0), indicating that the relative degree of sexual dimorphism changes with log(species size). (B) The same data represented as the ratio of log(Y_M/Y_F) plotted against log(species size). (C) Sexual dimorphism represented as the distance between size-standardized log-trait values for males and females: D_{SD}. (D) Sexual dimorphism represented as an index of the SD distance: $SDDI = \pm 1 \times D_{SD}$. In all panels, the dashed line corresponds to values representing no sexual dimorphism (the 1:1 line).**

the other sex, relative to overall size differences between species. In such cases, and based on the conceptual representation of Figure 2A, a slope higher than 1 would thus represent a situation where male size increases faster than female size, resulting in a trend where sexual dimorphism becomes more pronounced at large overall species sizes (see below). To evaluate these patterns statistically, a phylogenetic regression is performed to determine whether the slope differs from $\beta = 1.0$. Note that although both model I and model II regressions have been used previously, statistical biases resulting from the confounding of biological variation and measurement error make model II regression unsuitable for evolutionary analyses of allometric trends (see Hansen and Bartoszek 2012; Kilmer and Rodríguez 2017).

Using this procedure, interspecific trends that deviate from the 1:1 line (i.e., $\beta \neq 1.0$) indicate a significant allometric trend in SSD, where the relative degree of sexual dimorphism changes systematically with differences in species size. For instance, in male-biased species, slopes greater than 1.0 ($\beta > 1.0$) describe interspecific trends where larger species display disproportionately greater sexual dimorphism. Likewise, in female-biased species, a $\beta > 1.0$ indicates that smaller species display disproportionately greater levels of sexual dimorphism. In both cases, trends where $\beta > 1.0$ provide evidence consistent with Rensch's rule (Rensch 1960; Fairbairn 1997). In contrast, slopes significantly less than 1.0 ($\beta < 1.0$) represent the converse allometric pattern.

Under a distinct yet equivalent construction, patterns of sexual dimorphism may be interrogated using ratios of trait values: $\log(Y_M/Y_F)$. When plotted against log(species size) as in Figure 2B, the same information is conveyed as is found in the more commonly used $\log(Y_M)$ versus $\log(Y_M)$ plot of Figure 2A. However, in this alternative representation, the line

designating no sexual dimorphism is horizontal, with a slope of zero ($\beta = 0.0$) and an intercept of zero. As before, phylogenetic regression may be performed on these data, and in this case, interspecific patterns whose slope differs from zero ($\beta \neq 0.0$) represent allometric changes in sexual dimorphism. For instance, a slope greater than zero ($\beta > 0.0$) identifies a relative increase in sexual dimorphism in larger species (i.e., a trend consistent with Rensch's rule), while a slope less than zero ($\beta < 0.0$) reveals a relative decrease in sexual dimorphism with increasing species size. Finally, there are two important analytical aspects to note regarding this equivalency. First, Figure 2B does not represent a case where the independent variable is a component of the dependent variable (e.g., Y/X vs. X). Rather, the dependent variable in Figure 2B is the ratio of trait values in males and females ($\log(Y_M/Y_F)$) while the independent variable is species size. Second, if male and female trait values are first standardized to account for overall size (i.e., Mosimann shape variables: Mosimann 1970), the trait ratio remains unaltered because $\log(\frac{Y_M/\text{Size}}{Y_F/\text{Size}}) = \log(Y_M/Y_F)$. Thus, size standardization can easily be incorporated in this formulation: an important consideration for the next equivalency.

A third equivalency may be found by representing sexual dimorphism as a distance. This formulation recognizes the observation that male and female trait values represent points in a phenotypic dataspace. Species with little sexual dimorphism have similar male and female trait values (i.e., points closer together in the phenotypic space), while species exhibiting greater levels of sexual dimorphism have dissimilar male and female trait values (i.e., points that are further apart). Numerous studies have used distances to represent the degree of sexual dimorphism in phenotypic traits (e.g., Kaliontzopoulou et al. 2007; Testa and Dworkin 2016; Lisle and Rowe 2017; Yazdi and Alhajeri 2018, among others). Although prior studies have used various distance measures (e.g., Euclidean distance, Mahalanobis distance, etc.), here we use Euclidean distances obtained from size-standardized log-trait values: $D_{SD} = \sqrt{(\log(\frac{Y_M}{\text{Size}}) - \log(\frac{Y_F}{\text{Size}}))^2}$. The reason for this decision is that Euclidean distances obtained from Mosimann (1970) shape variables characterize the *relative* degree of sexual dimorphism, rather than the absolute difference between the sexes. Thus, larger values of D_{SD} represent a proportionately greater degree of phenotypic differentiation between the sexes, whereas smaller values represent proportionately less sexual dimorphism. Additionally, for univariate traits such as size, only D_{SD} obtained in this manner preserves the original trends of sexual dimorphism, as we describe next.

Figure 2C represents sexual dimorphism as this distance (D_{SD}) plotted against log(species size). This plot is similar to a Bland-Altman plot (Altman and Bland 1983), except that the Euclidean distance, rather than a difference score, is plotted along the *y*-axis. In our simulated example, there is an increase in the relative degree of sexual dimorphism at both large and small species sizes (Fig. 2C). This is because the data for this example were simulated such that the degree of sexual dimorphism increases in larger male-biased species as well as in smaller female-biased species. In such cases, the inflection point in Figure 2C represents a body size where there is no sexual dimorphism for the trait, and corresponds to the location where the $\log(M)$ versus $\log(F)$ regression line of Figure 2A crosses the 1:1 line representing no sexual dimorphism. This inflection point may represent the overall mean size across species in the lineage, or it may be some other value. For instance, in some lineages (e.g., turtles: Ceballos et al. 2013), nearly all species are female biased, in which case the inflection point for D_{SD} versus species size would be found at the far-right end of the plot.

Finally, from D_{SD} a *sexual dimorphism distance index* (*SDDI*) may be constructed as

$$SDDI = \pm 1 \times D_{SD}.$$

Here, D_{SD} is multiplied by either a $+1$ or -1, based on a comparison of male and female trait values for the species. For instance, for sexual dimorphism in body size, D_{SD} is multiplied by -1 for those species where females display larger values than males, and remains unchanged for species where males are larger than females. This logic is similar to that of Lovich and Gibbons (1992; see also Schutz et al. 2009) for their index of overall body size dimorphism. However, we multiply the D_{SD} of female-biased taxa by -1, rather than the converse, to retain the direction of the relationship displayed in Figure 2C with those in Figure 2B for consistency of interpretation. Note that from a geometric perspective, this procedure is tantamount to determining which species in Figure 2A are found below the 1:1 size line (i.e., the line representing no size dimorphism), and multiplying those species' D_{SD} by -1. Importantly, note that the pattern displayed in Figure 2D is identical to that of Figure 2B. This demonstrates the mathematical equivalency between Euclidean distances derived from Mosimann shape variables and log ratios of male and female trait values, which can therefore be used interchangeably for investigating variation in the degree of sexual dimorphism with respect to species size. For this reason, Euclidean distances on Mosimann shape variables are preferred to other distance measures for this application.

The equivalencies in Figure 2 are shown for univariate data, and as such are appropriate for describing the degree of sexual dimorphism in size, or any single-valued trait on a linear scale (e.g., wing length, horn size, etc.). Additionally however, the approach may be extended for use with multivariate data, as Euclidean distances may be derived for sets of continuous variables in any dimension. For p continuous traits, one finds the sexual dimorphism distance from the set of Mosimann shape variables as

$D_{SD} = \sqrt{\sum_{i=1}^{p}(\log(\frac{Y_{i,M}}{\text{Size}}) - \log(\frac{Y_{i,F}}{\text{Size}}))^2}$. Note that the set of multivariate traits must be measured in commensurate units (e.g., all traits measured on a linear scale), so that the resulting distances are interpretable (Adams and Collyer 2019). When this is not the case, one should convert the traits to their standard normal deviates prior to the calculation of the sexual dimorphism distance (see Legendre and Legendre 2012; Adams and Collyer 2019).

Unfortunately, applying the univariate logic used above to obtain *SDDI* from multidimensional data is more complicated, as sex-specific differences are not always guaranteed to align with some a priori direction in the multivariate dataspace. Thus, for multivariate datasets, one of two procedures may be used. First, for multivariate sets of traits that are measured on the same linear scale (e.g., length, width, and height measures), one could envision a hyperdimensional version of the plot displayed in Figure 2A, but where the set of male traits are plotted against the set of female traits. In this construction, because the traits are quantified on the same measured scale, the 1:1 size vector representing no sexual dimorphism does exist, and emanates from the origin of the space extending in a positive direction as the trait values increase. To determine whether male trait values deviate more from this vector than do female trait values, a partial least squares (PLS) analysis may be performed (Rohlf and Corti 2000). PLS is a multivariate association procedure that describes the covariation between sets of traits (in this case, between the set of male traits and the set of female traits). Scores along the first PLS axis represent the maximal covariation between male and female traits projected to a single dimension, and species whose male and female PLS scores are identical represent those that display no sexual dimorphism. Thus, deviations from that pattern represent instances of multivariate sexual dimorphism. By plotting these scores, one may determine which species display female scores (on PLS_1) that are larger than their corresponding male scores (when negative values on PLS_1 correspond to smaller individuals; otherwise, the converse comparison is used). The D_{SD} for these species may then be multiplied by -1 to obtain the *SDDI*. Note that when PLS is used on univariate data, this procedure provides values identical to those from the method described previously where male and female sizes are compared directly. Thus, for multivariate traits measured on a linear scale, this is a direct generalization of the standard univariate procedure.

Alternatively, one might be interested in examining multidimensional traits other than linear biometric measurements, such as color or shape. For instance, one may characterize the shape of males and females using geometric morphometric methods (Bookstein 1991; Mitteroecker and Gunz 2009; Adams et al. 2013), where the locations of anatomical landmarks and semilandmarks are used to obtain a set of shape variables. Geometric morphometric methods also result in a multidimensional characterization of phenotypic traits (standardized for size), from which the relative degree of sexual dimorphism for each species may be quantified using D_{SD}. However, because the resulting shape variables do not have a one to one correspondence with linear size measures, there is no a priori direction in the multivariate shape space that is equivalent to the 1:1 size vector found with sets of linear traits. In fact, for the case of isometry (i.e., shape does not change as size changes), all observations are represented by a single location in the shape space. Thus, although a PLS of male shapes versus female shapes will describe the covariation between them, this direction is not guaranteed to align with size because there is no direction in the shape space that may be used to unambiguously determine whether dimorphism is male or female biased. Nonetheless, one may still quantitatively determine whether the degree of SShD covaries with overall body size, using the sexual dimorphism index as defined by the dimorphism distance (i.e., $SDDI = D_{SD}$) to represent the degree of multivariate shape dimorphism for each species.

Once the *SDDI* has been calculated, *SDDI* may be plotted against log(species size) in the same manner as is shown in Figure 2D, and relative changes in multivariate sexual dimorphism as a function of size may be evaluated using phylogenetic regression. As before, the line representing no sexual dimorphism is a horizontal line centered on zero, as a distance of zero corresponds to no sexual dimorphism. Thus, a phylogenetic regression whose slope is significantly different from zero (i.e., $\beta \neq 0.0$) provides evidence for allometric changes in sexual dimorphism across species. For instance, a slope greater than zero ($\beta > 0.0$) identifies a relative increase in sexual dimorphism in larger species (i.e., a trend consistent with Rensch's rule), while a slope less than zero ($\beta < 0.0$) reveals a relative decrease in sexual dimorphism with increasing species size.

SIMULATIONS

To ascertain the statistical performance of the approach above, we conducted a series of computer simulations. We evaluated the ability of *SDDI* to characterize patterns of sexual dimorphism in both univariate and multivariate datasets. For each simulation, we generated a pure-birth phylogeny containing 50 species, on which we simulated datasets under a Brownian motion model of evolution. For univariate data ($p = 1$), a single trait was evolved along the phylogeny, representing the female trait values (x). Next, male trait values (y) were simulated in such a manner as to generate a known male:female relationship (plus random error), using the function: $y = x\beta + \mathcal{N}(\mu = 0, \sigma = 0.1)$. For type I error simulations, patterns of sexual dimorphism were generated such that there was no allometric trend in SSD, meaning that the relative degree of sexual dimorphism was random with respect to species size. To accomplish this we simulated male traits using $\beta = 1.0$,

which characterized a 1:1 relationship between male and female trait values and thus no systematic change in sexual dimorphism with changes in size. For power simulations, we simulated male values using $\beta = 1.15$, which resulted in a relative increase in the degree of sexual dimorphism as a function of size. A total of 1000 datasets were generated under each simulation condition. We then evaluated all datasets using standard approaches (i.e., a phylogenetic regression of log(male) values vs. log(female) as well as a phylogenetic regression of *SDDI* vs. log(species size)). The proportion of significant datasets was treated as the type I error (when $\beta = 1.0$) or power (when $\beta = 1.15$), respectively.

For multivariate data ($p = 5$), a slightly different procedure was used. First, both average body size (S) and the female trait values ($\mathbf{X}$) were simulated simultaneously on the phylogeny under Brownian motion, using a $(p + 1) \times (p + 1)$ trait covariance matrix ($\mathbf{R}$) with correlations between traits of ($r = 0.7$). Then, for simulations where there was no pattern of sexual dimorphism across species (i.e., type I error simulations), male trait values were generated by incorporating random error to the female trait values, in a manner analogous to that achieved in the univariate simulations: $\mathbf{Y} = \mathbf{X}_F + \mathcal{N}(\mu = 0, \sigma = \mathbf{R} \times 0.1)$. Next, for simulations where patterns of the degree of sexual dimorphism covaried with body size (i.e., power simulations), the multivariate relationship between female shape and body size was determined ($\mathbf{X} = S\mathbf{B} + \mathbf{E}$), from which the model coefficients ($\mathbf{X}$) and residuals ($\mathbf{E}$) were obtained. Male trait values were then generated by exaggerating the predicted relationship through multiplication of a scalar (1.15), and adding this to the residuals plus random error proportional to the degree of phenotypic change induced by the scalar: $\mathbf{Y} = (1.15 \times S\mathbf{B}) + \mathbf{E} + \mathcal{N}(\mu = 0, \sigma = \mathbf{R} \times 0.00001)$. This ensured that male and female trait values covaried with one another as expected, and that the relative degree of sexual dimorphism also covaried with size. As before, a total of 1000 datasets were generated under each simulation condition. We then evaluated all datasets using a phylogenetic regression of *SDDI* versus log(species size). The proportion of significant datasets was then treated as the type I error and power, respectively.

Simulation results: For the univariate dataset, we found that both a phylogenetic regression of male size on female size and a phylogenetic regression of *SDDI* on body size resulted in appropriate type I error rates near the nominal $\alpha \approx 0.05$ (Fig. 3). Further, when the simulated data contained a known allometric relationship between the degree of sexual dimorphism and species size, both procedures were capable of detecting the signal of the pattern, and did so with very high power. Thus, using the *SDDI* approach proposed here was equivalent to what is normally used for univariate datasets. Likewise, for multivariate data, the *SDDI* approach displayed appropriate type I error ($\alpha \approx 0.05$) and high statistical power under the conditions simulated (Fig. 3). Additionally, multiplying D_{SD} by ± 1 had little effect on the outcome

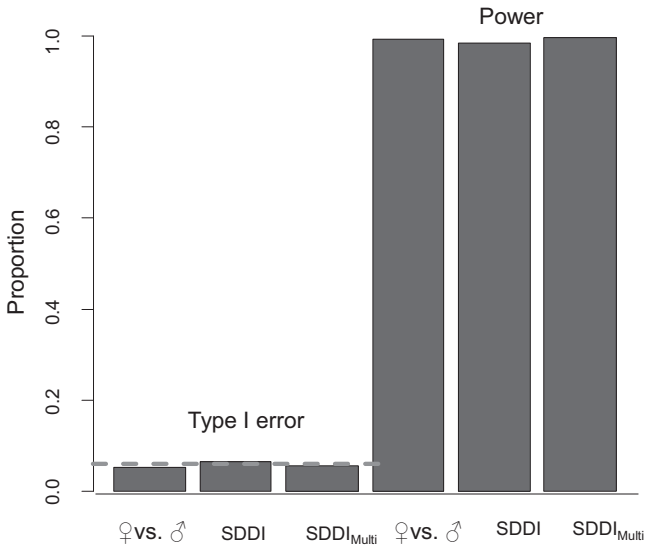


Figure 3. Results of phylogenetic simulations testing the type I error and statistical power for detecting allometric changes in the degree of sexual dimorphism in both univariate and multivariate traits. Vertical bars represent the proportion of datasets found to be significant. For type I error analyses, the dashed line marks the standard threshold of $\alpha = 0.05$. For univariate data, both phylogenetic regression of log(male) versus log(female) size, and *SDDI* versus log(species size) were performed. For multivariate data, only *SDDI* versus log(species size) was examined.

for multivariate data, as in both cases type I error and power results were virtually identical. Thus, methods for evaluating interspecific trends in sexual dimorphism using multivariate data are anticipated to remain robust for both sets of linear measurements treated as Mosimann (1970) shape variables, as well as other traits, such as shape variables derived from geometric morphometric methods. Overall results from these simulations imply that using the *SDDI* proposed here provides an appropriate means of characterizing allometric changes in the degree of sexual dimorphism across taxa in both univariate and multivariate traits, and that the procedure is capable of detecting patterns consistent with Rensch's rule (or its converse) when they are present in phenotypic datasets.

EMPIRICAL EXAMPLE

To illustrate the utility of the approach presented here, we conducted an analysis of both size and shape dimorphism in a group of Mediterranean lizards with extensive body size variation. Our dataset consisted of three data types: male and female values of body size (snout-vent length: SVL), male and female values for a series of head measurements (head length, head width, head height, pileus length, and mouth opening: Fig. 4A), and male and female values of head shape as described using geometric morphometrics (Fig. 4B). A total of 374 specimens from 21

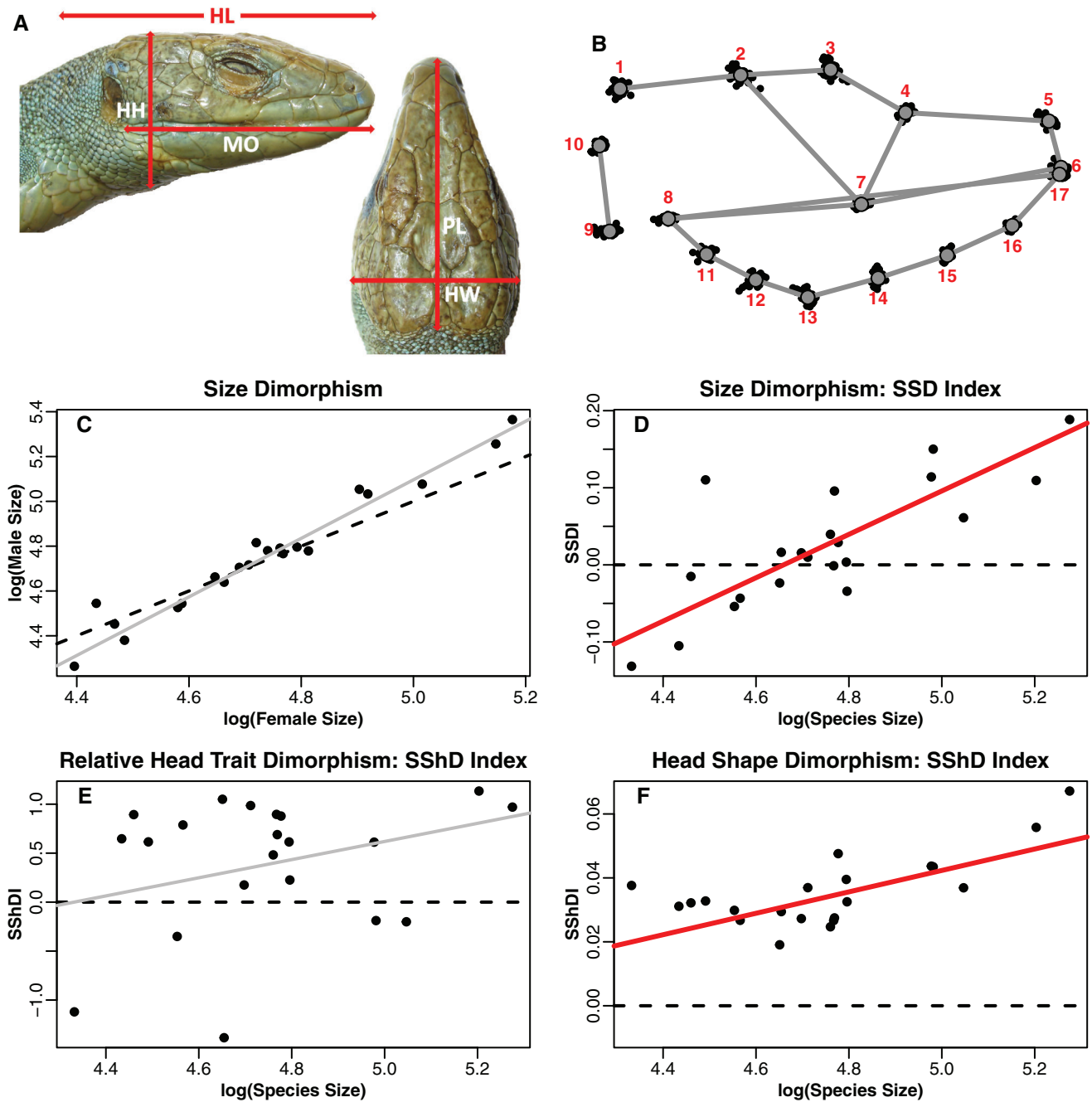


Figure 4. (A) Set of linear measurements used to obtain head proportions. HL, head length; HW, head width; HH, head height; PL, pileus length; MO, mouth opening. (B) Locations of 17 landmarks (1–10; 17) and semilandmarks (11–16) used to quantify head shape. (C) Patterns of sexual size dimorphism represented as log(male) versus log(female) size. (D) Patterns of sexual size dimorphism, represented as sexual size dimorphism index (*SSDI*) versus log(species size). (E) Multivariate patterns sexual dimorphism (*SShDI*) in Mosimann shape variables for head measurements versus log(species size). (F) Multivariate patterns of sexual shape dimorphism (*SShDI*) versus log(species size). In panels C, D, E, and F, the trend line indicates the regression estimate obtained from the data (red = significant, gray = not significant), while the dashed line corresponds to values representing no sexual dimorphism.

lineages of green lizards, a monophyletic clade that includes two genera (*Lacerta* and *Timon*), were obtained from natural history museum collections. For each lineage, we obtained samples distributed across the entire distribution range, resulting in an initial database of 1062 specimens. To take sampling bias into account, we selected the 10 largest individuals per sex, when sufficient specimens were available, for use in subsequent size and shape analyses.

From these specimens, we calculated mean body size for each sex and lineage. Likewise, we calculated the mean trait values for each sex and lineage for the set of linear measures. These values were then standardized by SVL; resulting in a set of head measurements proportional to body size for each sex × lineage combination (i.e., Mosimann 1970 shape variables). Additionally, we quantified lateral head shape variation using geometric morphometric methods (Adams et al. 2013). This was accomplished by first digitizing 17 landmarks and semilandmarks from images of the right side of the head (Fig. 4B). The thin-plate spline was used to estimate the position of missing landmarks (Gunz et al. 2009), and the position of the jaw relative to the skull was standardized using the fixed angle method (Adams 1999). Next, a generalized Procrustes analysis (Rohlf and Slice 1990) was performed to eliminate nonshape variation from the landmark data and align the specimens to a common coordinate system. The position of semilandmarks (i.e., 11–16, Fig. 4B) was optimized by minimizing the bending energy (Bookstein 1997). From the aligned Procrustes coordinates the mean head shape for males and for females was then calculated for each lineage (mean values for each lineage and sex for all linear biometric traits and for landmark coordinates are available in Supporting Information File 1). Finally, the phylogenetic relationships among lineages were estimated using published sequences on five mitochondrial and four nuclear gene fragments, totaling 8383 bp. These were then used following standard phylogenetic inference procedures to generate a dated consensus phylogeny for the lineages of interest (for details on phylogenetic reconstruction, see Supporting Information File 2).

Using these data, we conducted a series of analyses to investigate whether the degree of SSD and SShD differed systematically with overall body size in this group. First, we examined patterns of SSD using a phylogenetic regression of log(male) size against log(female) size. Additionally, we evaluated SSD patterns using the approach developed here, via a phylogenetic regression of the SSD index (*SDDI*) against log(body size) for each species. Second, we evaluated multivariate patterns of sexual dimorphism in head proportions in relation to body size, using the sexual dimorphism index obtained from the Euclidean distance between male and female trait value proportions (D_{SD}). PLS was used to determine which species displayed female scores (on PLS_1) larger than their corresponding male scores, and the sexual dimorphism index was then obtained by multiplying the sexual dimorphism distance by +1 or −1, respectively (i.e., $SDDI = \pm 1 \times D_{SD}$). We then performed a phylogenetic regression of *SDDI* for head proportions versus log(body size) to determine whether the relative degree of sexual dimorphism in head proportions changed systematically with differences in body size across species. Third, we obtained the degree of sexual dimorphism in head shape for each species using the Procrustes distance between male and female means, and from this calculated the SShD index (*SShDI*) in their original units as described above (i.e., $SShDI = D_{SD}$). We then performed a phylogenetic regression of SShD (*SShDI*) against log(body size) to determine whether the relative degree of head shape dimorphism changed systematically with differences in body size across species. Additionally, patterns of head shape dimorphism were further investigated using principal components analysis of the set of mean male and female head shapes across lineages. Finally, we used phylogenetic correlation (phylogenetic PLS: sensu Adams and Felice 2014) to determine whether the degree of head shape dimorphism was associated with levels of size dimorphism. All analyses were performed in R 3.6.2 (R Core Team 2019) using the packages `geomorph` (Adams and Otárola-Castillo 2013; Adams et al. 2019), `RRPP` (Collyer and Adams 2018), and routines written by the authors.

Empirical results: Using phylogenetic regression, we found a significant relationship between log(male) and log(female) size ($F = 286.14$, $Z = 3.03$, $P = 0.001$), with a slope greater than one, though not significantly so ($\beta = 1.31, T = 1.96, P = 0.062$: Fig. 4C). In general the evolutionary trend indicated that the degree of SSD differed with overall body size, such that in male-biased species the degree of sexual dimorphism increased at larger body sizes, and in female-biased species the degree of sexual dimorphism increased at smaller body sizes. Interestingly, when using the *SSDI* on the same data, we found a significant and positive evolutionary relationship between *SSDI* and log(body size), indicating that with this method, significant allometric changes in relative SSD were detected ($\beta = 0.28$, $F = 24.472$, $Z = 1.96$, $P = 0.001$: Fig. 4D). This allometric pattern across species was in the direction consistent with that expected for clades adhering to Rensch's rule.

When multivariate patterns of sexual dimorphism were evaluated using relative head dimensions, we found no allometric trend in the degree of sexual dimorphism relative to log(body size) ($F = 1.85$, $Z = 0.82$, $P = 0.194$: Fig. 4E). However, when sexual dimorphism in lateral head shape based on landmark-based shape data was investigated, there was a strong and significant relationship between the degree of SShD (*SShDI*) and log(body size) across taxa ($F = 13.54$, $Z = 1.65$, $P = 0.002$: Fig. 4F). This indicated that variation in lateral head shape displayed distinct differences between the sexes across species, whereas overall head proportions did not. A visual inspection of variation in lateral head shape dimorphism across species size (Fig. 4F) indicated that the relative degree of sexual dimorphism in head shape increased in larger species; a pattern consistent with what was expected under Rensch's rule. To our knowledge, this is the first empirical demonstration of an allometric trend in SShD being consistent with Rensch's rule for a multivariate dataset.

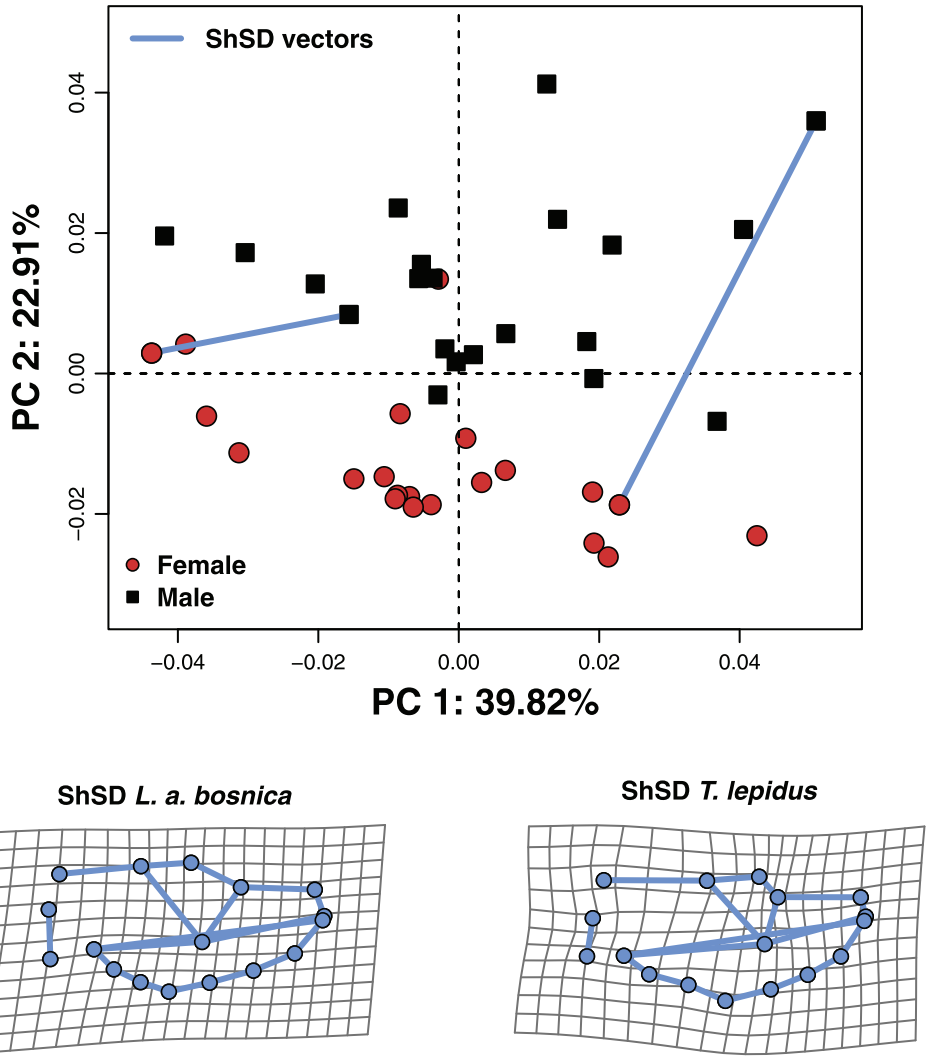


Figure 5. Principal components plot of male (black squares) and female (red points) species mean head shape: the first two PC axes explain over 60% of the total shape variation. Blue lines correspond to the sexual shape dimorphism in one of the smallest species, *Lacerta agilis bosnica*, and in the largest species, *Timon lepidus*. Thin-plate spline deformation grids display the mean head shape difference between males and females of these species.

Visualizing patterns of head shape dimorphism using principal components analysis facilitates the interpretation of such allometric patterns of sexual dimorphism (Fig. 5). Here, it was evident that males and females occupied distinct regions of morphospace. Further, the head shape differences between males and females of the smallest lineage, *Lacerta agilis bosnica*, were distinct from those of the largest species, *Timon lepidus*. When connected, the SShD vectors for these two species did not coincide with one another in the ordination, implying a difference in SShD across species. Specifically, the vector for *T. lepidus* was longer than that for *L. agilis bosnica*, which reflected the greater degree of SShD exhibited by this species. Thin-plate spline deformation grids facilitated a graphical description of these shape differences, where SShD in *L. agilis bosnica* was best described as a contrast between longer headed males, with an amplified tympanic area; and short-headed females, with a relatively more reduced tympanic region (Fig. 5, bottom left). By contrast, SShD in *T. lepidus* was both more prominent in the tympanic area, similar to what was observed in *L. agilis bosnica*; and also included a modification of the relative lower jaw area. Indeed, males of *T. lepidus* were characterized by both a longer posterior head region and by deeper lower jaw configurations as compared to females of the same species (Fig. 5, bottom right).

Finally, across taxa, the degree of body size and head shape dimorphism were significantly correlated with one another ($r = 0.57$, $P = 0.0068$), but not when evaluated in a phylogenetic context ($r_{PLS} = 0.167$, $Z = -0.122$, $P = 0.487$). Part of this

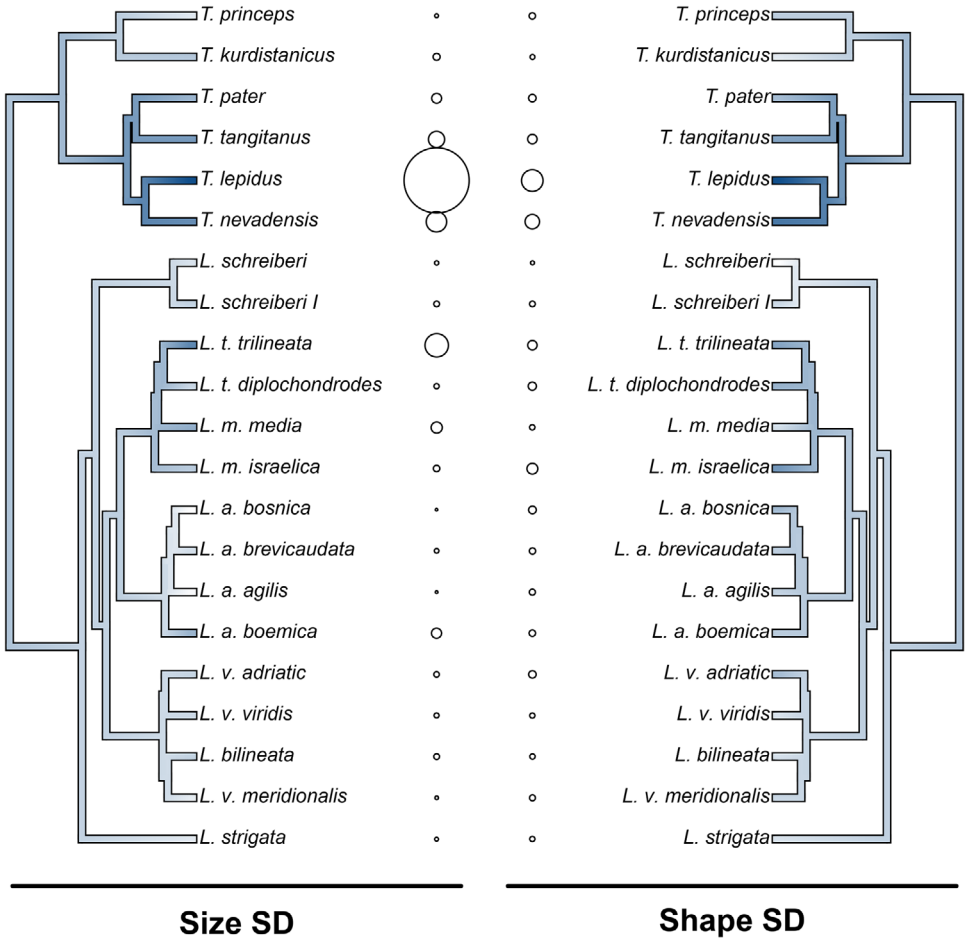


Figure 6. Heat maps (white: lower values; blue: higher values) displaying the evolution of (A) sexual size dimorphism, and (B) sexual shape dimorphism across the phylogeny. For each panel, an index of sexual size dimorphism (*SSDI*) or sexual shape dimorphism (*SShDI*) is displayed, with circles being proportional to the degree of sexual dimorphism.

difference may be explained by the fact that the largest species (i.e., members of the genus *Timon*), which also displayed the greatest degree of both size and shape dimorphism, form a clade within the broader phylogeny for the group (Fig. 6). Thus, despite the strong association of size and shape dimorphism, there were fewer changes of these patterns across branches of the phylogeny. Generally speaking, the degree of size dimorphism and the degree of shape dimorphism increased in larger taxa, and heat maps of the evolution of size and shape dimorphism across the phylogeny indicated a strong association between the two; particularly in large taxa (Fig. 6). Thus, in this system, it appeared that evolutionary changes in size differences between the sexes were accompanied by concomitant changes in head shape differences.

Discussion

A long-standing question in evolutionary biology is understanding why sexual dimorphism, the degree of differentiation between the sexes, varies across species. Frequently, it is of interest to explore whether the relative degree of sexual dimorphism changes allometrically as a function of overall body size (e.g., Rensch 1950; Abouheif and Fairbairn 1997; Fairbairn 1997). A common macroevolutionary trend in such studies is that the degree of sexual dimorphism increases with body size in species where males are the larger sex, and decreases with increasing body size in species where females are the larger sex; a pattern termed as Rensch's rule. Remarkably, virtually all recent studies have focused on macroevolutionary trends of allometric variation in SSD despite the clear functional relevance of sexual dimorphism in other traits (Fig. 1). This gap has been driven, in large part, by the paucity of analytical tools for evaluating allometric trends in sexual dimorphism in multivariate traits, such as color, ornament complexity, or shape. In this article, we fill this procedural gap by providing an analytical equivalency that allows the generalization of statistical tests of the allometry for sexual dimorphism in both univariate and multivariate traits. The approach describes the degree of sexual dimorphism as a relative distance between male and female trait values in phenotype space, thereby

facilitating its use on either single-valued traits (e.g., body size), or complex, multivariate traits (e.g., organismal shape). Computer simulations confirm that the approach exhibits appropriate type I error rates and statistical power, thereby providing an adequate procedure for testing whether empirical data display interspecific allometry for sexual dimorphism. The implementation of our approach on an empirical study of Mediterranean lizards revealed that allometric patterns of sexual dimorphism comply with Rensch's rule not only for body size, but also for head shape, offering new insights and triggering novel hypotheses about the possible proximate and evolutionary causes that may underlie such patterns.

Our empirical example in Mediterranean green lizards exemplifies a case study investigating variation in sexual dimorphism—not only in size—but also in multivariate phenotypes, like shape, and how this method can provide useful insights into the proximate and evolutionary causes underlying such patterns. First, we found that the degree of SSD increased as taxa became larger (Fig. 4C, D). This pattern is compliant with Rensch's rule and corresponds with hyperallometry (Abouheif and Fairbairn 1997), which is to be expected when males are the larger sex (Fairbairn 1997). In this group males are larger than females in most lineages (Fig. 4C), as is commonly observed in lacertids (Braña 1996). Additionally, as in many lizard species, sexual selection in this group is primarily mediated through territoriality, where male-male competition selects for a larger male body size (Stamps 1983). Thus, in this system there is an association between male-biased SSD and male-male competition. As such, the patterns of size dimorphism observed in this study are consistent with those expected under a scenario where sexual selection drives the evolution of larger male body size across taxa via male antagonistic interactions.

Likewise, our multivariate analyses revealed that head morphology differed between the sexes, and that allometric trends in the degree of sexual dimorphism in multivariate head shape also corresponded with what was expected under Rensch's rule (Fig. 4F). That is, although both small (e.g., *L. agilis bosnica*, Fig. 5, left) and large (e.g., *T. lepidus*, Fig. 5, right) species are sexually dimorphic in head shape, the degree of SShD increases with average body size (Fig. 4F); a pattern consistent with a scenario of hyperallometry. Interestingly, although this pattern was identified using head shape variables derived from geometric morphometric methods, such a pattern was not identified when examining relative head dimensions, for which a much larger dispersion of species-specific values of sexual dimorphism was observed (Fig. 4E). This may reflect the capacity of geometric morphometric techniques for capturing functionally relevant, fine-scale variation in morphology, as opposed to the more coarse-grained information provided by linear measurements (see, e.g., Adams and Rohlf 2000; Fabre et al. 2014). Indeed, the examination of variation across shape space revealed that sexual dimorphism in head morphology was associated with an amplification of the posterior head region, and also in the relative size of the lower jaw (in the case of *T. lepidus*), which might not be sufficiently captured by the linear measurements examined here. Biomechanically, these are precisely the anatomical regions where the jaw adductor muscles reside (Haas 1973), and as such, an amplification of these areas in males would enhance biting performance (Herrel et al. 1996; Kaliontzopoulou et al. 2012); a functional trait that has important implications for male competitive capacity (Huyghe et al. 2005; Lailvaux and Irschick 2007). In addition, one might predict that the need for stronger jaw musculature in males becomes disproportionately more intense with increasing body size, as male combats are expected to be more fierce among larger bodied opponents. Thus, our findings that head shape dimorphism increases with overall body size is also consistent with the hypothesis that sexual selection on structures related to territoriality and male competitive interactions are responsible for the macroevolutionary patterns of SShD observed in this group. To our knowledge, this is the first example of Rensch's rule in a multivariate phenotype.

With respect to the analytical approach proposed here, our characterization of sexual dimorphism via a *multivariate distance* and the *SDDI* statistic is completely general, and may be used to evaluate evolutionary trends in any continuous, quantitative trait that differs between the sexes. Our empirical example highlighted the efficacy of the approach for evaluating trends in univariate traits such as body size, and also several types of complex data where organismal phenotypes are quantified by multiple dimensions. As such, the approach developed here expands our current analytical toolkit to provide a means of evaluating evolutionary trends in sexual dimorphism for a broader class of phenotypic traits than has previously been considered. Indeed, this advance more closely embodies Rensch's (1950) original conceptualization for understanding patterns of sexual dimorphism, as his broader vision was to explain why phenotypic differences *writ large* exist among the sexes (Fig. 1). Thus, use of the *SDDI* will facilitate a greater degree of evolutionary exploration into patterns of sexual dimorphism than has been possible in recent decades. Further, with the inclusion of multivariate traits, the formulation proposed here opens the door for investigations into the evolution of SShD, and whether allometric trends in the degree of sexual dimorphism of multivariate phenotypes correspond to those expected under Rensch's rule. Thus, the mathematical procedure proposed here is general, and may be used for any quantitative phenotypic trait under scrutiny.

Finally, because *SDDI* is derived from a phenotypic distance, one could, in theory, use the approach to characterize patterns of sexual dimorphism in non-continuous traits, and determine quantitatively whether the degree of sexual dimorphism is

enhanced with increasing body size. Across the tree of life, major phenotypic adaptations are often described as evolutionary innovations or novelties (sensu Wagner and Altenberg 1996; Wagner and Muller 2002; Peterson and Müller 2016), where these changes are characterized as discrete shifts from one phenotypic state to another (e.g., Holliday and Gardner 2012; O'Keefe et al. 2011). In like manner, discrete phenotypic differences are known to exist between the sexes; for instance where males display horns or other ornamentation (Geist and Bayer 1988; Emlen 2008) that females lack. Over evolutionary time, a series of such discrete phenotypic differences may accumulate in males relative to females, resulting in an elaboration of phenotypic differences between the sexes in suites of such traits. With an appropriate distance measure for discrete traits (e.g., Hamming distance), the approach developed here is capable of characterizing such patterns, and determining whether sets of discrete phenotypic differences are enhanced with increasing body size among species. Thus, our approach is the first to our knowledge to facilitate a formal evaluation of both discrete and continuous phenotypic differences between the sexes, providing a comprehensive means of determining whether sets of phenotypic traits differ allometrically across taxa, and in a manner as predicted by Rensch's rule.

AUTHOR CONTRIBUTIONS

DCA devised the approach, AK provided the empirical example; all authors contributed to all parts of this manuscript.

ACKNOWLEDGMENTS

We thank E. Baken, M. Collyer, B. Juarez, and N. Valenzuela for comments on drafts of this manuscript; Ana Perera, Inés Freitas, and Daniele Salvi for the phylogeny reconstruction; and Chiara Ripa and Zélia Pereira for aiding shape data acquisition. This work was sponsored in part by National Science Foundation Grant DBI-1902511 (to DCA), and by FEDER Funds through the Operational Competitiveness Factors Program—COMPETE and National Funds through FCT—Foundation for Science and Technology within the scope of the project "PTDC/BIA-EVL/28090/2017-POCI-01-0145-FEDER-028090" (to AK). Empirical data collection was supported by several SYNTHESYS grants of the European Union to AK (FR-TAF-6534, CZ-TAF-6587, GB-TAF-5330, ES-TAF-5876). We thank the curators of the herpetological collections of the Estación Biológica de Doñana (Sevilla), the Museo Nacional de Ciencias Naturales (Madrid), the Muséum national d'Histoire naturelle (Paris), the National History Museum of London, the Naturhistorische Museum Wien, the National Museum of Prague, the Zoological Research Museum Alexander Koenig (Bonn), and the Zoologische Staatssammlung (Munich) for facilitating access to specimens of green lizards.

DATA ARCHIVING

Data will be made available on DRYAD upon publication (https://doi.org/10.5061/dryad.fttdz08qd).

LITERATURE CITED

Abouheif, E., and D. J. Fairbairn. 1997. A comparative analysis of allometry for sexual size dimorphism: assessing Rensch's rule. Am. Nat. 149:540–562.

Adams, D. C. 1999. Methods for shape analysis of landmark data from articulated structures. Evol. Ecol. Res. 1:959–970.

Adams, D. C., and M. L. Collyer. 2018. Multivariate phylogenetic comparative methods: evaluations, comparisons, and recommendations. Syst. Biol. 67:14–31.

———. 2019. Phylogenetic comparative methods and the evolution of multivariate phenotypes. Annu. Rev. Ecol. Evol. Syst. 50:405–425.

Adams, D. C., and R. N. Felice. 2014. Assessing trait covariation and morphological integration on phylogenies using evolutionary covariance matrices. PLoS ONE 9:e94335.

Adams, D. C., and E. Otárola-Castillo. 2013. Geomorph: an R package for the collection and analysis of geometric morphometric shape data. Methods Ecol. Evol. 4:393–399.

Adams, D. C., and F. J. Rohlf. 2000. Ecological character displacement in *plethodon*: biomechanical differences found from a geometric morphometric study. Proc. Natl. Acad. Sci. USA 97:4106–4111.

Adams, D. C., F. J. Rohlf, and D. E. Slice. 2013. A field comes of age: geometric morphometrics in the 21st century. Hystrix 24:7–14.

Adams, D. C., M. L. Collyer, and A. Kaliontzopoulou. 2019. Geomorph: software for geometric morphometric analyses. R package version 3.1.1. Available at https://cran.r-project.org/package=geomorph. Accessed February 15, 2019.

Altman, D. G., and J. M. Bland. 1983. Measurement in medicine: the analysis of method comparison studies. Statistician 32:307–317.

Andersson, M. 1994. Sexual selection. Princeton Univ. Press, Princeton, NJ.

Astúa, D. 2010. Cranial sexual dimorphism in new world marsupials and a test of Rensch's rule in *Didelphidae*. J. Mammal. 91:1011–1024.

Badyaev, A. V. 2002. Growing apart: an ontogenetic perspective on the evolution of sexual size dimorphism. Trends Ecol. Evol. 17:369–378.

Berns, C. M., and D. C. Adams. 2013. Becoming different but staying alike: patterns of sexual size and shape dimorphism in bills of hummingbirds. Evol. Biol. 40:246–260.

Blanckenhorn, W. U., R. C. Stillwell, K. A. Young, C. W. Fox, and K. G. Ashton. 2006. When Rensch meets Bergmann: does sexual size dimorphism change systematically with latitude? Evolution 60:2004–2011.

Blanckenhorn, W. U., A. F. G. Dixon, D. J. Fairbairn, M. W. Foellmer, P. Gibert, K. van der Linde, R. Meier, S. Nylin, S. Pitnick, C. Schoff, et al. 2007. Proximate causes of Rensch's rule: does sexual size dimorphism in arthropods result from sex differences in development time? Am. Nat. 169:245–257.

Blows, M. W. 2007. A tale of two matrices: multivariate approaches in evolutionary biology. J. Evol. Biol. 20:1–8.

Bolnick, D. I., and M. Doebeli. 2003. Sexual dimorphism and adaptive speciation: two sides of the same ecological coin. Evolution 57:2433–2449.

Bonduriansky, R. 2007. Sexual selection and allometry: a critical appraisal of the evidence and ideas. Evolution 61:838–849.

Bookstein, F. L. 1991. Morphometric tools for landmark data: geometry and biology. Cambridge Univ. Press, Cambridge.

———. 1997. Landmark methods for forms without landmarks: morphometrics of group differences in outline shape. Med. Image. Anal. 1:225–243.

Braña, F. 1996. Sexual dimorphism in *Lacertid* lizards: male head increase vs female abdomen increase? Oikos 75:511–523.

Burbrink, F. T., and I. Futterman. 2019. Female-biased gape and body-size dimorphism in the new world watersnakes (tribe: *Thamnophiini*) oppose predictions from Rensch's rule. Ecol. Evol. 9:9624–9633.

Butler, M. A., and J. B. Losos. 2002. Multivariate sexual dimorphism, sexual selection, and adaptation in greater antillean *Anolis* lizards. Ecol. Monogr. 72:541–559.

Butler, M. A., T. W. Schoener, and J. B. Losos. 2000. The relationship between sexual size dimorphism and habitat use in greater antillean *Anolis* lizards. Evolution 54:259–272.

Butler, M. A., S. A. Sawyer, and J. B. Losos. 2007. Sexual dimorphism and adaptive radiation in *Anolis* lizards. Nature 447:202–205.

Ceballos, C. P., D. C. Adams, J. B. Iverson, and N. Valenzuela. 2013. Phylogenetic patterns of sexual size dimorphism in turtles and their implications for Rensch's rule. Evol. Biol. 40:194–208.

Collyer, M. L., and D. C. Adams. 2018. RRPP: an R package for fitting linear models to high-dimensional data using residual randomization. Methods Ecol. Evol. 9:1772–1779.

Collyer, M. L., D. J. Sekora, and D. C. Adams. 2015. A method for analysis of phenotypic change for phenotypes described by high-dimensional data. Heredity 115:357–365.

Cox, R. M., S. L. Skelly, and H. B. John-Alder. 2003. A comparative test of adaptive hypotheses for sexual size dimorphism in lizards. Evolution 57:1653–1669.

Dale, J., P. O. Dunn, J. Figuerola, T. Lislevand, T. Székely, and L. A. Whittingham. 2007. Sexual selection explains Rensch's rule of allometry for sexual size dimorphism. Proc. R. Soc. B 274:2971–2979.

Darwin, C. R. 1871. The descent of man, and selection in relation to sex. J. Murray, London.

Dayan, T., and D. Simberloff. 2005. Ecological and community-wide character displacement: the next generation. Ecol. Lett. 8:875–894.

De Lisle, S. P., and L. Rowe. 2013. Correlated evolution of allometry and sexual dimorphism across higher taxa. Am. Nat. 182:630–639.

Emlen, D. J. 2008. The evolution of animal weapons. Annu. Rev. Ecol. Evol. S. 39:387–413.

Endler, J. A. 1983. Natural and sexual selection on color patterns in Poeciliid fishes. Environ. Biol. Fish. 9:173–190.

Fabre, A.-C., R. Cornette, K. Huyghe, D. V. Andrade, and A. Herrel. 2014. Linear versus geometric morphometric approaches for the analysis of head shape dimorphism in lizards. J. Morphol. 275:1016–1026.

Fairbairn, D. J. 1997. Allometry for sexual size dimorphism: pattern and process in the coevolution of body size in males and females. Annu. Rev. Ecol. Evol. Syst. 28:659–687.

———. 2013. Odd couples—extraordinary differences between the sexes in the animal kingdom. Princeton Univ. Press, Princeton, NJ.

Fairbairn, D. J., and R. F. Preziosi. 1994. Sexual selection and the evolution of allometry for sexual size dimorphism in the water strider, *Aquarius remigis*. Am. Nat. 144:101–118.

Fairbairn, D. J., W. U. Blanckenhorn, and T. Székely. 2007. Sex, size and gender roles. Oxford Univ. Press, Oxford.

Garcia-Navas, V., T. Bonnet, R. Bonal, and E. Postma. 2015. The role of fecundity and sexual selection in the evolution of size and sexual size dimorphism in new world and old world voles (Rodentia: Arvicolinae). Oikos 125:1250–1260.

Geist, V., and M. Bayer. 1988. Sexual dimorphism in the cervidae and its relation to habitat. J. Zool. 214:45–53.

Gidaszewski, N. A., M. Baylac, and C. P. Klingenberg. 2009. Evolution of sexual dimorphism of wing shape in the *Drosophila melanogaster* subgroup. BMC Evol. Biol. 9:110.

Gunz, P., P. Mitteroecker, S. Neubauer, G. W. Weber, and F. L. Bookstein. 2009. Principles for the virtual reconstruction of hominin crania. J. Hum. Evol. 57:48–62.

Haas, G. 1973. Muscles of the jaws and associated structures in the Rhynchocephalia and Squamata. Pp. 285–490 *in* C. Gans and T. S. Parsons, eds. Biology of the reptilia, Vol. 4. Academica Press, Washington, DC.

Hansen, T. F., and K. Bartoszek. 2012. Interpreting the evolutionary regression: the interplay between observational and biological errors in phylogenetic comparative studies. Syst. Biol. 61:413–425.

Herrel, A., R. V. Damme, and F. D. Vree. 1996. Sexual dimorphism of head size in *Podarcis hispanica atrata*: testing the dietary divergence hypothesis by bite force analysis. Netherlands J. Zool. 46:253–262.

Hirst, A. G., and T. Kiørboe. 2014. Macroevolutionary patterns of sexual size dimorphism in copepods. Proc. R. Soc. B 281:20140739.

Holliday, C. M., and N. M. Gardner. 2012. A new eusuchian crocodyliform with novel cranial integument and its significance for the origin and evolution of crocodylia. PLoS ONE 7:e30471.

Horne, C. R., A. G. Hirst, and D. Atkinson. 2020. Selection for increased male size predicts variation in sexual size dimorphism among fish species. Proc. R. Soc. B 287:20192640.

Huyghe, K., B. V. Hooydonck, H. Scheers, M. Molina-Borij, and R. V. Damme. 2005. Morphology, performance and fighting capacity in male lizards, *Gallotia galloti*. Funct. Ecol. 19:800–807.

Johnson, P. J., M. J. Noonan, A. C. Kitchener, L. A. Harrington, C. Newman, and D. W. Macdonald. 2017. Rensching cats and dogs: feeding ecology and fecundity trends explain variation in the allometry of sexual size dimorphism. R. Soc. Open Sci. 4:170453.

Kaliontzopoulou, A., M. A. Carretero, and G. A. Llorente. 2007. Multivariate and geometric morphometrics in the analysis of sexual dimorphism variation in *Podarcis* lizards. J. Morphol. 268:152–165.

———. 2010. Intraspecific ecomorphological variation: linear and geometric morphometrics reveal habitat-related patterns within *Podarcis bocagei* wall lizards. J. Evol. Biol. 23:1234–1244.

Kaliontzopoulou, A., D. C. Adams, A. van der Meijden, A. Perera, and M. A. Carretero. 2012. Relationships between head morphology, bite performance and ecology in two species of *Podarcis* wall lizards. Evol. Ecol. 26:825–845.

Kaliontzopoulou, A., M. A. Carretero, and D. C. Adams. 2015. Ecomorphological variation in male and female wall lizards and the macroevolution of sexual dimorphism in relation to habitat use. J. Evol. Biol. 28:80–94.

Kelly, C. D., K. E. Folinsbee, D. C. Adams, and M. D. Jennions. 2013. Intraspecific sexual size and shape dimorphism in an Australian freshwater fish differs with respect to a biogeographic barrier and latitude. Evol. Biol. 40:408–419.

Kilmer, J. T., and R. L. Rodríguez. 2017. Ordinary least squares regression is indicated for studies of allometry. J. Evol. Biol. 30:4–12.

Lailvaux, S. P., and D. J. Irschick. 2007. The evolution of performance-based male fighting ability in caribbean *Anolis* lizards. Am. Nat. 170:573–586.

Lande, R. 1979. Quantitative genetic analysis of multivariate evolution, applied to brain: body size allometry. Evolution 33:402–416.

Lande, R., and S. J. Arnold. 1983. The measurement of selection on correlated characters. Evolution 37:1210–1226.

Laporte, M., P. Berrebi, J. Claude, D. Vinyoles, Q. Pou-Rovira, J.-C. Raymond, and P. Magnan. 2017. The ecology of sexual dimorphism in size and shape of the freshwater blenny *Salaria fluviatilis*. Curr. Zool. 64:183–191.

Law, C. J., and R. S. Mehta. 2018. Carnivory maintains cranial dimorphism between males and females: evidence for niche divergence in extant musteloidea. Evolution 72:1950–1961.

Legendre, P., and L. Legendre. 2012. Numerical ecology. 3rd ed. Elsevier, Amsterdam.

Lisle, S. P. D., and L. Rowe. 2017. Disruptive natural selection predicts divergence between the sexes during adaptive radiation. Ecol. Evol. 7:3590–3601.

Littleford-Colquhoun, B. L., C. Clemente, G. Thompson, R. H. Cristescu, N. Peterson, K. Strickland, D. Stuart-Fox, and C. H. Frere. 2019. How sexual and natural selection shape sexual size dimorphism: evidence from multiple evolutionary scales. Funct. Ecol. 33:1446–1458.

Lovich, J. E., and J. W. Gibbons. 1992. A review of techniques for quantifying sexual size dimorphism. Growth Dev. Aging 56:269–281.

Meiri, S., A. E. Kadison, M. Novosolov, P. Pafilis, J. Foufopoulos, Y. Itescu, P. Raia, and D. Pincheira-Donoso. 2014. The number of competitor species is unlinked to sexual dimorphism. J. Anim. Ecol. 83:1302–1312.

Mitteroecker, P., and P. Gunz. 2009. Advances in geometric morphometrics. Evol. Biol. 36:235–247.

Mosimann, J. E. 1970. Size allometry: size and shape variables with characterizations of the lognormal and generalized gamma distributions. J. Am. Stat. Assoc. 65:930–945.

O'Higgins, P., D. R. Johnson, W. J. Moore, and R. M. Flinn. 1990. The variability of patterns of sexual dimorphism in the hominoid skull. Experientia 46:670–672.

O'Keefe, F. R., H. P. Street, B. C. Wilhelm, C. D. Richards, and H. Zhu. 2011. A new skeleton of the cryptoclidid plesiosaur *Tatenectes laramiensis* reveals a novel body shape among plesiosaurs. J. Vertebr. Paleontol. 31:330–339.

Östman, O., and D. Stuart-Fox. 2011. Sexual selection is positively associated with ecological generalism among agamid lizards. J. Evol. Biol. 24:733–740.

Peñalver-Alcázar, M., P. Galán, and P. Aragón. 2019. Assessing Rensch's rule in a newt: roles of primary productivity and conspecific density in interpopulation variation of sexual size dimorphism. J. Biogeogr. 46:2558–2569.

Peterson, T., and G. B. Müller. 2016. Phenotypic novelty in EvoDevo: the distinction between continuous and discontinuous variation and its importance in evolutionary theory. Evol. Biol. 43:314–335.

Punzalan, D., and L. Rowe. 2015. Evolution of sexual dimorphism in phenotypic covariance structure in phymata. Evolution 69:1597–1609.

R Core Team. 2019. R: a language and environment for statistical computing. R Foundation for Statistical Computing, Vienna, Austria.

Regis, K. W., and J. M. Meik. 2017. Allometry of sexual size dimorphism in turtles: a comparison of mass and length data. PeerJ 5:e2914.

Reiss, M. J. 1986. Sexual dimorphism in body size: are larger species more dimorphic? J. Theor. Biol. 121:163–172.

Rensch, B. 1950. Die abhangigkeit der relativen sexualdifferenz von der korpergrosse. Bonner Zoologische Beitraege 1:58–69.

———. 1960. Evolution above the species level. Columbia Univ. Press, New York.

Rohlf, F. J., and M. Corti. 2000. The use of partial least-squares to study covariation in shape. Syst. Biol. 49:740–753.

Rohlf, F. J., and D. E. Slice. 1990. Extensions of the Procrustes method for the optimal superimposition of landmarks. Syst. Zool. 39:40–59.

Sanger, T. J., E. Sherratt, J. W. McGlothlin, E. D. Brodie III, J. B. Losos, and A. Abzhanov. 2013. Convergent evolution of sexual dimorphism in skull shape using distinct developmental strategies. Evolution 67:2180–2193.

Schutz, H., P. D. Polly, J. D. Krieger, and R. P. Guralnick. 2009. Differential sexual dimorphism: size and shape in the cranium and pelvis of grey foxes (*Urocyon*). Biol. J. Linn. Soc. 96:339–353.

Serrano-Meneses, M.-A., and T. Szekely. 2006. Sexual size dimorphism in seabirds: sexual selection, fecundity selection and differential niche-utilisation. Oikos 113:385–394.

Stamps, J. 1983. Sexual selection, sexual dimorphism and territoriality. Pp. 169–204 *in* R. B. Huey, E. R. Pianka, and T. W. Schoener, eds. Lizard ecology: studies of a model organism. Harvard Univ. Press, Cambridge, MA.

Stephens, P. R., and J. J. Wiens. 2009. Evolution of sexual size dimorphisms in emydid turtles: ecological dimorphism, Rensch's rule, and sympatric divergence. Evolution 63:910–925.

Stuart-Fox, D. 2008. A test of Rensch's rule in dwarf chameleons (*Bradypodion* spp.), a group with female-biased sexual size dimorphism. Evol. Ecol. 23:425–433.

Stuart-Fox, D., and A. Moussalli. 2007. Sex-specific ecomorphological variation and the evolution of sexual dimorphism in dwarf chameleons (*Bradypodion* spp.). J. Evol. Biol. 20:1073–1081.

Tarr, S., S. Meiri, J. J. Hicks, and A. C. Algar. 2018. A biogeographic reversal in sexual size dimorphism along a continental temperature gradient. Ecography 42:706–716.

Testa, N. D., and I. Dworkin. 2016. The sex-limited effects of mutations in the egfr and tgf-β signaling pathways on shape and size sexual dimorphism and allometry in the *Drosophila* wing. Dev. Genes Evol. 226:159–171.

Wagner, G. P., and L. Altenberg. 1996. Perspective: complex adaptations and the evolution of evolvability. Evolution 50:967.

Wagner, G. P., and G. B. Muller. 2002. Evolutionary innovations overcome ancestral constraints: a re-examination of character evolution in male sepsid flies (Diptera: Sepsidae). Evol. Dev. 4:1–6.

Watson, N. L., and L. W. Simmons. 2010. Mate choice in the dung beetle *Onthophagus sagittarius*: are female horns ornaments? Behav. Ecol. 21:424–430.

Wyman, M. J., J. R. Stinchcombe, and L. Rowe. 2013. A multivariate view of the evolution of sexual dimorphism. J. Evol. Biol. 26:2070–2080.

Yazdi, F. T., and B. H. Alhajeri. 2018. Sexual dimorphism, allometry, and interspecific variation in the cranial morphology of seven meriones species (Gerbillinae, Rodentia). Hystrix 29:162–167.

Associate Editor: M. Zeldith
Handling Editor: A. McAdam

Supporting Information

Additional supporting information may be found online in the Supporting Information section at the end of the article.

Supplementary Table 1: Lineages considered for the full and reduced, after applying the cutting point of 2.5MYA, datasets, and GenBank accession numbers for each gene fragment used.